Onboard Approximation of Dynamic Load-Response Relationship of Track Structure Using Laser Doppler Vibrometer and Axle Box Accelerometer

Zeng, Yuanchen; Núñez, Alfredo; Li, Zili

DOI
10.1109/I2MTC62753.2025.11079168

Publication date
2025

Document Version
Final published version

Published in
IEEE International Instrumentation and Measurement Technology Conference, I2MTC 2025 - Proceedings

2025 IEEE International Instrumentation and Measurement Technology Conference (I2MTC) | 979-8-3315-0500-4/25/$31.00 ©2025 IEEE | DOI: 10.1109/I2MTC62753.2025.11079168

Onboard Approximation of Dynamic Load-Response Relationship of Track Structure Using Laser Doppler Vibrometer and Axle Box Accelerometer

Yuanchen Zeng
Section of Railway Engineering
Delft University of Technology
Delft, The Netherlands
Y.Zeng-2@tudelft.nl

Alfredo Núñez
Section of Railway Engineering
Delft University of Technology
Delft, The Netherlands
A.A.NunezVicencio@tudelft.nl

Zili Li
Section of Railway Engineering
Delft University of Technology
Delft, The Netherlands
Z.Li@tudelft.nl

***Abstract*—This paper proposes an onboard measurement technology that combines a Laser Doppler Vibrometer (LDV) and an Axle Box Accelerometer (ABA) to approximate the dynamic load-response relationship of railway tracks. Unlike existing track-side and onboard technologies, this paper eliminates the need for load measurement, estimation, or control, enabling continuous measurements under operational conditions. The LDV mounted on the moving vehicle captures the track vibration response contactlessly, while the wheel vibration measured by ABA is used to directly represent the dynamic vehicle load. The LDV and ABA signals are combined to approximate the load-response relationship in the frequency domain. Experimental validation on a vehicle-track test rig demonstrates the effectiveness of the developed system at different speeds. Further comparisons with the hammer test result confirm its ability to capture the local dynamic properties of consecutive track segments along a railway track and also its superiority in measurement efficiency. This paper offers a promising solution for monitoring railway tracks on a large scale and allowing prescriptive maintenance of rail infrastructures.**

Keywords—Laser Doppler Vibrometer, Axle Box Accelerometer, railway track, frequency response function, hammer test

I. Introduction

A dynamic load-response relationship describes how a structure resists dynamic excitations. It is defined as the ratio of the dynamic deformation and/or motion to the applied dynamic load, and such ratios are frequency-dependent. For railway track structures, it is often known as frequency response functions and receptance/mobility/accelerance functions [1], which carry the dynamic properties of various track components and indicate their health conditions. They can be used to quantify degradation, detect defects, and analyze root causes. Monitoring such dynamic load-response relationships is essential for the safety and quality of train operations as well as the effective and efficient decisions of track maintenance.

Conventionally, the dynamic load-response relationship of track structures is measured through impact modal tests using either impact hammers or falling weights [2]–[4]. These tests involve generating an artificial impact on a track structure (usually on rails) to excite its dynamic behaviors. The applied load is typically measured by a force transducer within the excitation device, while the vibration responses at targeted locations are typically measured with accelerometers. The measured forces and responses enable the estimation of the frequency response functions of the measured track structure. Though reliable, with high coherence and low noise, these tests are labor-intensive and time-consuming, limiting their practicality for large-scale applications. Additionally, artificial loads cannot fully excite track dynamics experienced under actual train loads.

Alternatively, special measurement vehicles for onboard monitoring of such dynamic load-response relationships have been developed [5][6]. These vehicles typically apply oscillatory loads to rails through wheels and measure the resulting dynamic responses through wheel movements [7]. Such technologies allow continuous measurement of dynamic load-response relationships along a railway track but only at a pre-defined frequency. The running speed and the excitation frequency are limited to control the wheel load, and the high costs associated with the manufacturing, operation, and maintenance of such vehicles limit their frequent use.

In [8], an onboard solution is proposed to measure dynamic load-response relationships of tracks using operational vehicle loads. It integrates a Laser Doppler Vibrometer (LDV) and accelerometers on the vehicle. The LDV contactlessly scans the track structure and measures its vibration in response to the moving vehicle. At the same time, the accelerometers measure the vehicle vibrations, which are used to update a vehicle model and estimate the dynamic wheel-rail force. The measured track response and the estimated force are further used to estimate the dynamic load-response relationship. This solution works with operational loads and excitations. However, the measurement of the full vehicle vibration and the process of vehicle model updating and wheel-rail force estimation introduce significant complexities and uncertainties, particularly when applied to trains with multiple wheels.

Building on [8], this paper aims to simplify the instrumentation and eliminate the need for vehicle model updating and load estimation. We make use of the wheel vibration measured by Axle Box Accelerometer (ABA) to directly represent the dynamic vehicle load on track structures [9][10]. The ABA and LDV signals are further combined to calculate transfer functions that approximate dynamic load-response relationships of track structures. We conduct laboratory experiments, including comparisons with traditional hammer tests, to evaluate the effectiveness and efficiency of the

This research is supported by ProRail and the project RESET (Reliable Embankments for Safe Expansion in Rail Traffic)

developed technology in capturing the local dynamic properties of consecutive track segments along a railway track.

Subsequently, Sections II and III present the proposed methodology and the experimental validation, respectively, and the conclusions are drawn in Section IV.

II. The Proposed Methodology

A. Instrumentation Design

The proposed measurement system is illustrated in Fig. 1. An LDV is mounted on the vehicle with its laser directed onto a track structure. An accelerometer is mounted on the axle box, known as ABA. The laser spot of the LDV may be offset from the wheel position. As the vehicle travels along and interacts with the track, the ABA measures the vibration of the wheel (axle box) due to wheel-rail contact, while the LDV measures the vibration of the track in response to the moving excitation. To compensate for the vibration of the LDV itself, an additional accelerometer is mounted on the LDV.

Both LDV and ABA offer high compatibility with various types of vehicles due to their compact sizes and independence from load or speed control. In practical applications, an LDV can be mounted on a bogie frame [11], outside a car body [12], or inside a car body [13], depending on mounting and protection design, power supply, as well as the permissible vibration intensity and stand-off distance of the LDV. For vehicles equipped with ABAs or other supplementary sensors (e.g., GPS or tachometer), combining the LDV channel with the existing monitoring system is often possible, although proper synchronization may be required. In terms of cost consideration, the proposed system requires investment in the LDV. Still, its benefit in providing insights into the load-response relationships of railway tracks can potentially result in long-term cost savings by enabling early fault detection and prescriptive maintenance.

A railway track is typically a continuous structure with discrete supports, exhibiting dynamic properties that vary across different locations. To capture such variations and characterize local properties, we divide a track structure into consecutive segments, as illustrated in Fig. 1. Within each segment, the measured LDV and ABA signals are used to approximate the dynamic load-response relationship specific to that segment.

B. Approximation Method

Let $y(t)$ denote the LDV signal segment (in the unit of velocity) when its laser scans a certain track segment, while $x(t)$ and $a(t)$ denote the ABA signal and LDV accelerometer signal

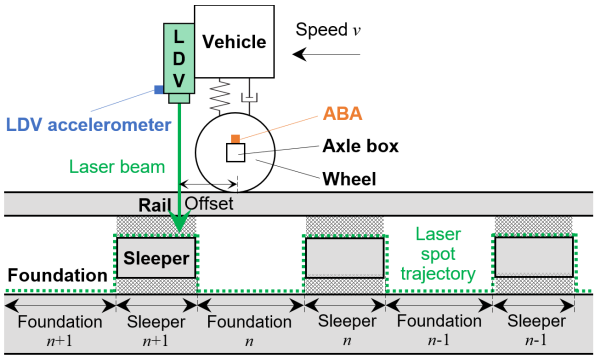

Fig. 1. Instrumentation design and track segmentation.

(in the unit of acceleration) over the same time period, respectively. In this paper, we use the transfer function from the wheel vibration to the track response to approximate the dynamic load-response relationship of a track structure.

Continuous LDV scanning on rough track surfaces inevitably introduces speckle noise into LDV signals due to the formation and rapid change in speckle patterns [13]. Speckle noise distorts LDV signals with irregular spikes and varies with the scanning speed. Speckle noise must be mitigated to ensure accurate analysis of vibration behaviors. To address this, we apply the method in [13] to detect and replace data points in $y(t)$ affected by speckle noise. This method is designed to perform effectively across different scanning speeds. We denote the LDV signal after speckle noise mitigation as $y^*(t)$.

The ABA signal $x(t)$ and the processed LDV signal $y^*(t)$ are the primary input and output for approximating the dynamic load-response relationship of the measured track segment, respectively. Involving also the cancellation of the disturbance from the LDV vibration $a(t)$, the approximator for the dynamic load-response relationship is expressed as follows,

$$H(f)=\frac{P_{(\int x)(y^*-\int a)}(f)}{P_{(\int x)(\int x)}(f)} \tag{1}$$

where f represents frequency, $P_{pq}(f)$ denotes the cross-spectral density between $p(t)$ and $q(t)$ and reduces to the auto-spectral density when $p(t)=q(t)$. Therefore, the dynamic load-response relationship is approximated using an H1 estimator of the transfer function from the ABA to the LDV, i.e., the ratio of the cross-spectral density between the LDV and the ABA to the auto-spectral density of the ABA. The H1 estimator is chosen because the LDV signal is generally noisier than the ABA signal. In this process, the LDV vibration is canceled out from the LDV signal, and the ABA signal is integrated into velocity, resulting in a dimensionless load-response relationship.

Given the linearity of Fourier transform and the integration in the frequency domain, (1) can be further written as follows,

$$\begin{aligned} H(f)&=\frac{P_{(\int x)(y^*)}(f)}{P_{(\int x)(\int x)}(f)}-\frac{P_{(\int x)(\int a)}(f)}{P_{(\int x)(\int x)}(f)} \\ &=\frac{(2\pi fi)P_{xy^*}(f)}{P_{xx}(f)}-\frac{P_{xa}(f)}{P_{xx}(f)} \end{aligned} \tag{2}$$

where i denotes the imaginary unit.

Based on (2), the dynamic load-response relationship of each track segment can be approximated using the signals measured on that segment. Analytically, a load-response relationship is a function of frequency. In numerical computation, due to the truncation, each calculated load-response relationship is a vector of complex numbers corresponding to discrete frequencies. Notably, both the cancellation of the LDV vibration disturbance and the integration are performed in the frequency domain, eliminating the need for time-domain processing.

C. Parameter Selection

The key parameters in the above process are the window length, window type, and overlap ratio in the spectral analysis. Among these, the window length and type are crucial for balancing spectral resolution, variance, and leakage.

The window length is mainly constrained by the number of data points available per track segment and the required spectral resolution. Let L_s denote the length of a track segment, v the train speed, f_s the sampling rate, and Δf_{max} the lowest acceptable frequency resolution. The window length N_w should be selected within the following range.

$$\frac{f_s}{\Delta f_{max}} \le N_w \le \frac{L_s}{v} f_s \tag{3}$$

Different window types have different main-lobe widths and side-lobe levels, affecting the accuracy of spectral analysis. A narrower main lobe generally provides better separation between closely spaced peaks, but this usually comes with larger side lobes, leading to poorer leakage suppression [14]. Among a variety of window functions, the Hann window is considered a general-purpose choice that balances the resolution and leakage.

Overlapping can further reduce variances, noise, and information loss in spectral analysis. An overlap ratio greater than 50% is recommended to obtain smooth results.

III. Experimental Validation

A. Experimental Setup

We implement the proposed instrumentation design on the V-Track test rig at TU Delft [15], as shown in Fig. 2. The test rig resembles a simplified vehicle moving along a scaled track structure. The springs in the vehicle provide a static vertical force through pre-compression and also act as a suspension system to reduce vibration transmission. The sprung part of the vehicle is connected to a rotational platform, while the unsprung part, including an axle box and a wheel, directly interacts with the track structure. The scaled track structure consists of a rail supported discretely by sleepers on top of a foundation slab. For each sleeper, rail fasteners and a rail pad provide stiffness in connection to the rail, and sleeper bolts and a sleeper pad provide stiffness in connection to the foundation slab.

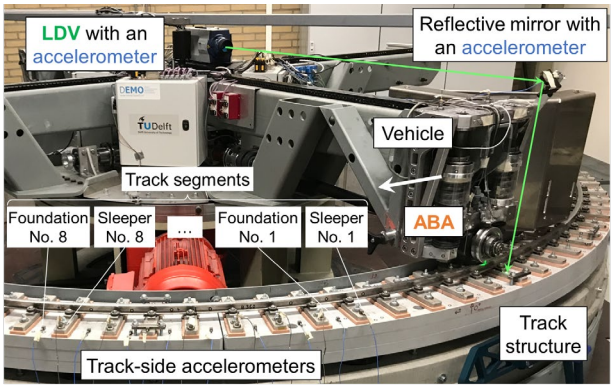

Fig. 2. Experimental setup on the TU Delft V-Track test rig.

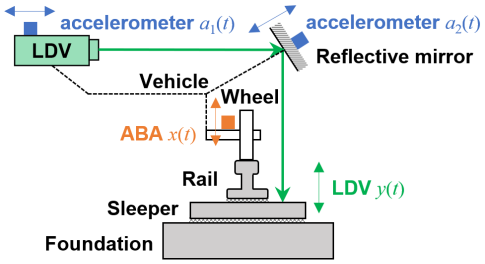

Fig. 3. Illustration of the instrumentation.

Fig. 3 provides a detailed illustration of the instrumentation setup. An LDV is mounted at the center of the test rig with its laser beam directed onto the track structure surface via a reflective mirror mounted on the vehicle. An ABA is mounted on the vehicle axle box. When the vehicle moves along the track, the wheel rolls over the rail, exciting the vibration of the track structure. Simultaneously, the LDV continuously scans the track structure. The dynamic loading from the wheel to the track is represented by the ABA measurement, and the dynamic response of the track is measured by the LDV.

To eliminate the influence of the LDV and mirror vibrations on the LDV signal, accelerometers are mounted on both the LDV and the mirror to measure their vibrations along the laser beam directions, denoted as $a_1(t)$ and $a_2(t)$, respectively. The combined influence of their vibrations on the LDV signal is expressed as follows,

$$a(t) = w_1 a_1(t) + w_2 a_2(t) \tag{4}$$

where w_1 and w_2 are the scaling factors depending on the orientation of the LDV and the mirror. In our test setup, w_1=1 and w_2=1.15. Based on (4), (2) can be rewritten as follows.

$$H(f) = \frac{(2\pi fi) P_{xy^*}(f)}{P_{xx}(f)} - w_1 \frac{P_{xa_1}(f)}{P_{xx}(f)} - w_2 \frac{P_{xa_2}(f)}{P_{xx}(f)} \tag{5}$$

The discrete support of the rail by the assemblies of fasteners, sleepers, and sleeper pads makes it necessary to separate their local properties when monitoring the entire track structure. To accomplish this, we divide the track structure into consecutive segments, as shown in Figs. 1 and 2. These segments include both sleeper and foundation segments, numbered sequentially. Accordingly, the LDV and accelerometer signals are segmented based on the position of the laser spot, which is obtained using the angular position of the vehicle on the rotational platform and accounting for the laser-wheel offset.

When testing the developed monitoring technology, the static wheel load is 4 kN, and the speed v ranges from 4 km/h to 10 km/h. Multiple runs are performed at each speed. The laser spot of the LDV is behind the wheel-rail contact point with an offset of approximately 1/3 of the sleeper spacing. The sampling rate of the LDV and accelerometer signals is f_s=102.4 kHz.

B. Verification of the Onboard LDV

To verify the effectiveness of the onboard LDV in measuring the track vibrations, we also instrument 16 consecutive track segments (Sleeper No.1, Foundation No. 1, Sleeper No. 2, …, Foundation No. 8) with track-side accelerometers. Measurements are conducted simultaneously by both the

onboard and the track-side systems, and the measured track vibrations are compared between the two systems. Before performing the comparison, speckle noise in the LDV signals is mitigated, and the LDV and mirror vibrations are removed, as described by $y^*(t) - w_1 \int a_1(t)\,dt - w_2 \int a_2(t)\,dt$. Additionally, to focus on the dominant frequencies of the track structure, both the LDV and the track-side accelerometer signals are filtered with a 50~2000 Hz band-pass filter.

Fig. 4 shows the comparison results for two of the segments measured at the vehicle speeds of 4 km/h and 10 km/h. The processed LDV signals are in good agreement with the track-side accelerometer signals. While the signal length is shorter at the higher vehicle speed, the consistency between the two sensors increases due to the larger vibration amplitude. These results demonstrate the effectiveness and accuracy of the onboard LDV in measuring the track vibrations, as well as the successful mitigation of speckle noise and cancellation of the LDV and mirror vibrations. This performance is achieved without the need to adjust the parameters of the algorithm for different speeds, showing its effectiveness across speeds.

C. *Approximation of Dynamic Load-response Relationships*

The proposed load-response relationship approximation method is then applied to the onboard measurements at different speeds and across multiple runs. Hann windows with a 95% overlap ratio are used for the spectral analysis. Given that the time length for measuring a track segment varies with the running speed, window lengths are adjusted according to the speed. The key information of the signal analysis is listed in Table 1. As expected, the frequency resolution becomes worse at a higher speed due to the shorter signal length.

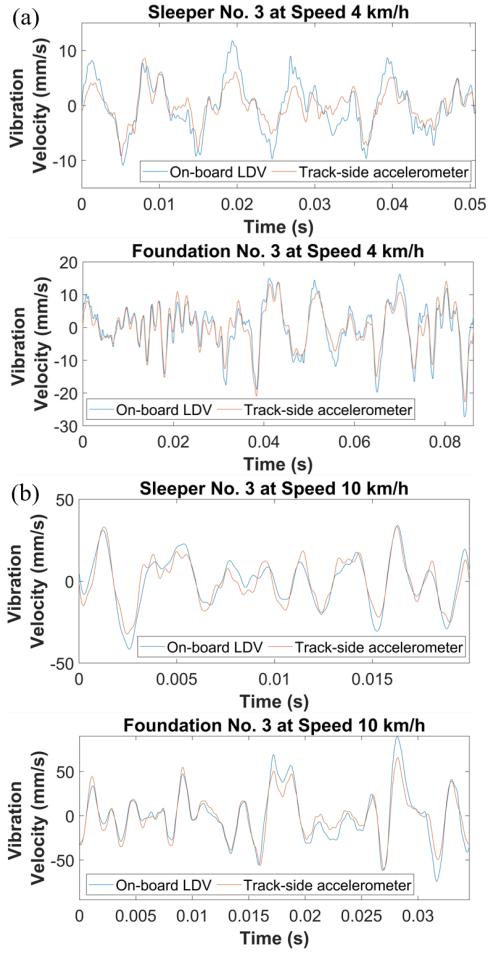

Fig. 4. Track vibrations measured by the onboard LDV and the track-side accelerometers on Sleeper No.3 and Foundation No. 3. (a) At the speed of 4 km/h; (b) At the speed of 10 km/h.

Each obtained load-response relationship is a vector of complex numbers corresponding to discrete frequencies. We take the logarithm of their absolute values and average them across different runs at each speed. The results at 4 km/h, covering the 16 instrumented track segments (from Sleeper No.1 to Foundation No. 8), are plotted as a spectrogram in Fig. 5 (a). In this plot, each foundation segment occupies twice the space of a sleeper segment, considering their actual size ratio (see Fig. 3). In general, as the frequency increases, the magnitude of the load-response relationship becomes larger. The local peak and dip regions suggest potential resonance and anti-resonance behaviors, respectively. For example, a pronounced peak region can be observed near the foundation slab gap in Foundation No. 4 (see Fig. 3), characterized by high peaks at 400–600 Hz and a broader frequency profile extending down to 200 Hz.

The results at 6~10 km/h are shown in Fig. 5 (b)~(d), using a consistent color mapping across the speeds. Similar patterns can be observed in these spectrograms, such as the prominent peak regions near Foundation No. 4 and other regions marked by the white boxes. Such similarities show that the load information, represented by the ABA signals, effectively normalizes the different amplitudes of the track response at different speeds. However, variations also emerge across the different speeds. For example, dip regions around 600 Hz near Sleeper No. 5~8 are observed at 6~10 km/h but are absent at 4 km/h, likely because the lower speed does not sufficiently excite such high-frequency vibrations. Additionally, noise and errors inherent in the spectral analysis of short signals also contribute to variations in the results. Additionally, we analyze the influence of the overlap ratio and find that the spectrogram pattern becomes stable as the overlap ratio increases, confirming the strategy of using a ratio greater than 50% in Section II.C.

D. *Validation with Impact Hammer Tests*

To verify the above approximation results, we conduct impact hammer tests on the same track structure, as shown in Fig. 6. To account for the laser-wheel offset of the onboard measurement, we generate an impact force on the rail head at a similar offset for each track-side accelerometer. The impact force of the hammer and the impact response of the accelerometer are measured, taped with a force window and an exponential window, respectively, and then used to estimate an accelerance function. Accelerance is chosen to represent the load-response relationship because the division of acceleration (in m/s^2) by force (in $N=kg{\cdot}m/s^2$) can cancel out m/s^2 and leave $1/kg$, which is more comparable to the dimensionless approximation from the onboard measurement using (1).

The hammer test and the estimation of accelerance are conducted for each of the 16 instrumented track segments. For each track segment, the test is repeated five times, and the estimation results are averaged. Fig. 7 shows the accelerance functions over these track segments using also a spectrogram.

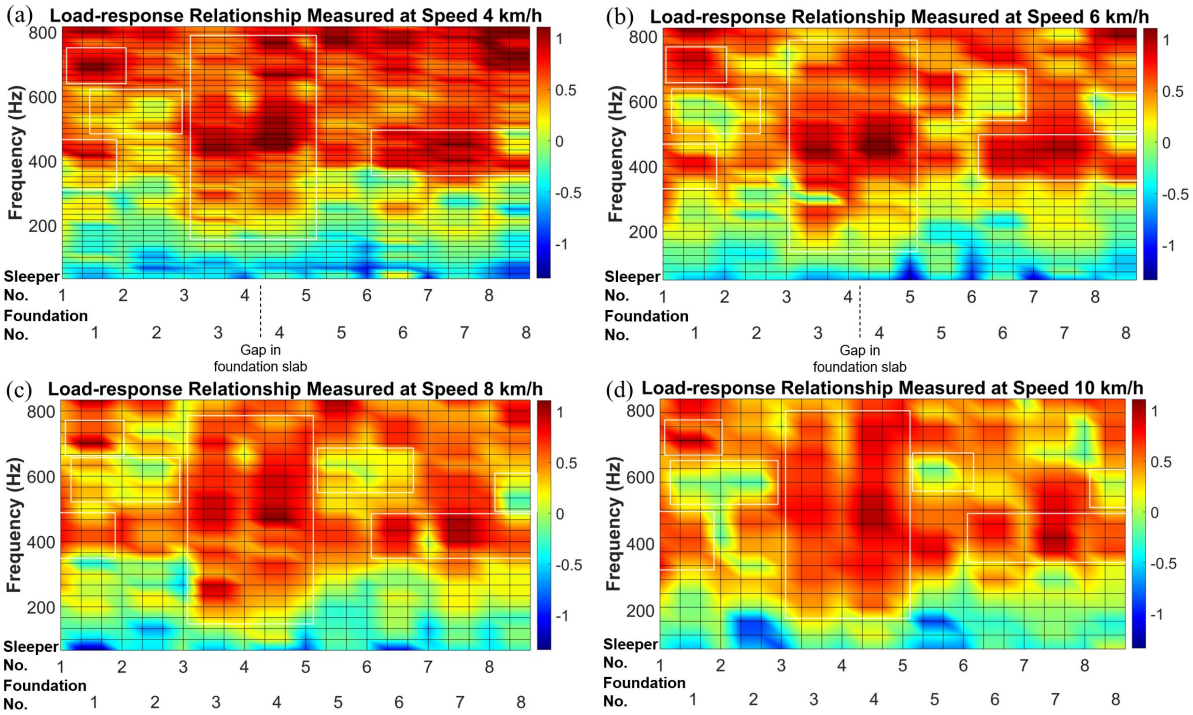

Fig. 5. Approximated dynamic load-response relationships over the instrumented track segments. (a) At the speed of 4 km/h; (b) At the speed of 6 km/h; (c) At the speed of 8 km/h; (d) At the speed of 10 km/h.

TABLE I. SIGNALS MEASURED AT DIFFERENT SPEEDS

Speed v	Number of runs	Time length*	Window lengths N_w		Frequency resolution Δf
			Sleeper segment	*Foundation segment*	
4 km/h	7	0.91 s	3072 points	6144 points	33.3 / 16.7 Hz
6 km/h	5	0.61 s	2048 points	4096 points	50 / 25 Hz
8 km/h	9	0.45 s	1536 points	3072 points	66.7 / 33.3 Hz
10 km/h	6	0.36 s	1228 points	2456 points	83.4 / 41.7 Hz

*over the entire instrumented track segments per run

The findings from comparing Fig. 7 with the results in Fig. 5 of the onboard measurement are given below.

- Due to the longer signal length in the hammer tests than in the onboard measurement and the lower noise level, the frequency resolution of the hammer test results (1.56 Hz) is higher than the onboard results, and the spectrogram is smoother and less noisy.
- Similar patterns can be observed between Fig. 5 and Fig. 7 at different locations and frequencies, such as the peak region with the broader frequency profile near the gap in the foundation slab, as well as other peak and dip regions marked by the white boxes. This consistency demonstrates that the onboard technology effectively approximates the local load-response relationship of the track structure over a wide range of frequencies.
- Among the four speeds tested, the speeds of 6 km/h and 8 km/h provide better agreement with the hammer test results. The possible reason is that the track dynamics are effectively excited at these speeds, and the signal length remains sufficient for reasonable spectral resolution. In contrast, at 4 km/h, the track may not be sufficiently excited, while at 10 km/h, the shorter signal length per track segment leads to poorer frequency resolution.
- Deviations can be observed between the onboard and the hammer test results, partially due to the different working conditions. In the onboard measurement, both the wheel and laser spot are moving, and the track is loaded by the vehicle. Conversely, in the hammer tests, both the hammer and the accelerometer positions are fixed, and the track is unloaded.

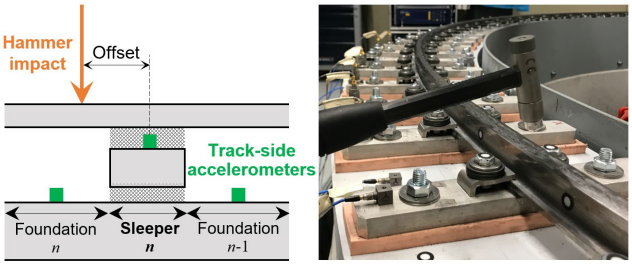

Fig. 6. Impact hammer tests on the instrumented track segments.

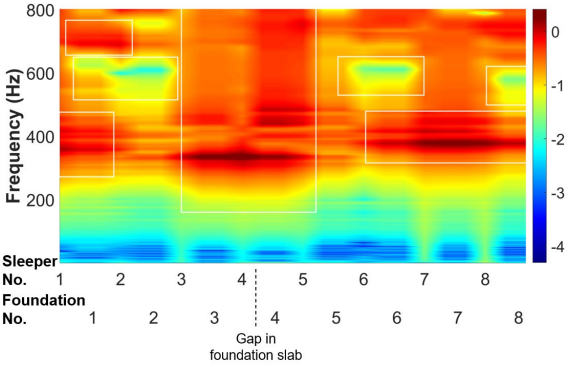

Fig. 7. Accelerance functions from the impact hammer tests.

TABLE II. COMPARISON WITH HAMMER TEST

Aspects	The developed onboard monitoring technology	Traditional hammer tests
Accuracy	Approximate dynamic load-response relationship when a track is loaded; speckle noise; low resolution; lack of force normalization.	Measure dynamic load-response relationship when a track is unloaded; low noise; high resolution.
Cost	High investment in equipment.	High labor costs and risks for manual set-up and excitations.
Time	Efficient; minimal disturbance to train traffic.	Disruption to train traffic.
Applicability	Suitable for large scale.	Localized.

- The proposed onboard measurement method is much faster than the hammer tests. At the speed of 6 km/h, it takes 0.6 seconds per run to cover the 16 track segments. In contrast, it takes hours to install the track-side accelerometers and then conduct the impact hammer tests segment by segment. A general comparison between the developed technology and traditional hammer tests is made in Table 2. Such difference is even more pronounced when considering large-scale railway tracks in the real field, for example, the Dutch rail network with a total length of over 3,200 km. A train equipped with the developed technology can cover the entire network within days, whereas it is impractical to perform hammer tests along the network. More importantly, onboard measurements can be performed regularly, or even daily if integrated into passenger trains, to characterize the degradation of track structures. This underscores the potential of the developed technology for large-scale monitoring and predictive maintenance.

IV. CONCLUSIONS

This paper develops and tests a novel monitoring technology for approximating the dynamic load-response relationships of track structures. The major conclusions are as follows.

- The track vibration measured by the LDV varies significantly at different vehicle speeds. The consistency in the approximation results across the different speeds underscores the value of using the ABA to represent the dynamic vehicle load and to normalize the track response.
- The match between the onboard measurement result and the hammer test result demonstrates the effectiveness of the developed technology in approximating the load-response relationship of the track structure over a broad range of frequencies and capturing the local dynamic properties of the consecutive track segments.
- In comparison to existing technologies, the developed system eliminates the need for load measurement, estimation, or control. Its high efficiency potentially allows frequent and large-scale railway track monitoring.

Our future research will focus on refining the approximation method and expanding its validation scale. The limitations of signal segmentation and spectral analysis will be overcome by developing more adaptive methods. The methodology will be further tested in conditions with varying vehicle speeds, where the ABA signal may be affected by traction or barking forces and speed variations can lead to time-variant resolution in frequency. Full-scale field tests will be conducted to verify the developed technology under real-world conditions. These developments will further enhance the practicability of this technology for structural health monitoring and prescriptive maintenance of rail infrastructures.

ACKNOWLEDGMENT

The authors thank Jan Moraal and Fang Ren for supporting the test on the test rig.

REFERENCES

[1] A. C. Lamprea-Pineda, D. P. Connolly, A. Castanheira-Pinto, P. Alves-Costa, M. F. Hussein, and P. K. Woodward, "On railway track receptance," Soil Dyn. Earthq. Eng., vol. 177, 108331, February 2024.

[2] M. Oregui, Z. Li, and R. Dollevoet, "Identification of characteristic frequencies of damaged railway tracks using field hammer test measurements," Mech. Syst. Signal Process., vol. 54–55, pp. 224–242. March 2015.

[3] S. Unsiwilai, C. Shen, Y. Zeng, L. Wang, A. Núñez, and Z. Li, "Vertical dynamic measurements of a railway transition zone: a case study in Sweden," J. Civ. Struct. Health Monit., vol. 14, pp. 979–996, February 2024.

[4] Y. Bai, Z. He, S. Qu, X. Wang, P. Li, X. Zhang, and W. Zhai, "Rail pad damping characteristics in track vibration reduction evaluated through hammer tests and theoretical analysis," Meas., vol. 239, 115467, January 2025.

[5] P. Wang, L. Wang, R. Chen, J. Xu, J. Xu, and M.Gao, "Overview and outlook on railway track stiffness measurement," J. Mod. Transp., vol. 24, pp. 89–102, May 2016.

[6] Y. Tong, G. Liu, K. Yousefian, and G. Jing, "Track vertical stiffness–value, measurement methods, effective parameters and challenges: A review," Transp. Geotech., vol. 37, 100833, November 2022.

[7] E. Berggren, Railway Track Stiffness: Dynamic Measurements and Evaluation for Efficient Maintenance, Stockholm: KTH, doctoral dissertation, 2009.

[8] Y. Zeng, A. Núñez, and Z. Li, "Measuring transfer functions of track structures in a test rig with laser Doppler vibrometer and accelerometers on a moving vehicle," Mech. Syst. Signal Process., vol. 214, 111392, May 2024.

[9] Y. Ji, J. Zeng, and W. Sun, "Research on wheel-rail local impact identification based on axle box acceleration," Shock Vib., vol. 2022, 3226253, January 2022.

[10] Z. Yang, and Z. Li, "Wheel-rail dynamic interaction," In Rail Infrastructure Resilience, Cambridge: Woodhead Publishing, 2022, pp. 111–135.

[11] K. Kaynardag, G. Battaglia, A. Ebrahimkhanlou, A. Pirrotta, and S. Salamone, "Identification of bending modes of vibration in rails by a laser Doppler vibrometer on a moving platform," In Exp. Tech., vol. 45, pp. 13–24, September 2021.

[12] C. Yang, K Kaynardag, and S. Salamone, Missing rail fastener detection based on laser Doppler vibrometer measurements," In J. Nondestruct. Eval., vol. 42, 68, July 2023.

[13] Y. Zeng, A. Nunez, and Z. Li, "Railway sleeper vibration measurement by train-borne laser Doppler vibrometer and its speed-dependent characteristics," Comput.-Aided Civ. Infrastruct. Eng., vol. 39, no. 16, pp. 2408–2426, August 2024.

[14] G. Heinzel, A. Rüdiger, and R. Schilling, "Spectrum and spectral density estimation by the discrete Fourier transform (DFT), including a comprehensive list of window functions and some new at-top windows," 2002, Online: https://pure.mpg.de/rest/items/item_152164/component/file_152163/content

[15] M. Naeimi, Z. Li, R. H. Petrov, J. Sietsma, and R. Dollevoet, "Development of a new downscale setup for wheel-rail contact experiments under impact loading conditions," Exp. Tech., vol. 42, pp. 1–17, February 2018.